Vol. 06, No. 3 (2024) 1309-1316, doi: 10.24874/PES.SI.24.03.007

Proceedings on Engineering Sciences

www.pesjournal.net

NUMERICAL EXPLORATION OF VISCOUS FLOW REGIMES: INSIGHTS FROM POISEUILLE, COUETTE AND TAYLOR-COUETTE FLOWS

Venkat Rao Kanuri
K. V. Chandra Sekhar
P. S. Brahmanandam[1]
M. S. R. Murthy

Received 16.10.2023.
Received in revised form 17.11.2023.
Accepted 12.12.2023.
UDC – 519.876.5

Keywords:

Analytical and numerical solutions, Poiseuille flow, Couette flow, Pressure gradient force, Flow around a circular cylinder, Velocity profile

A B S T R A C T

We present a numerical study for Poiseuille and Couette as well as Taylor-Couette swirling flows. The governing equations of momentum and energy are transformed into coupled and nonlinear ordinary differential equations using similarity transformation and then solved numerically. We critically evaluate the effect of dimensionless pressure gradients on fluid velocity and observed that the velocity increases as the dimensionless pressure gradient increases. Couette flows are simulated in different scenarios, including top plate moving, bottom plate moving, and top plate moving in adverse pressure gradient conditions. In a third scenario, the flow velocity profile revealed a backflow regime (BFR). A simple schematic model is, therefore, proposed to explain the presence of BFR in the flow's profile. Numerical and analytical solutions around the circular cylinder are presented. The marginal discrepancy between the analytical and numerical profiles is maximum at ~ 90^0 and 270^0 degrees, which indicates that the chosen method is suitable and capable of reproducing engineering problems. Velocity magnitude and vector diagrams show that the cylinder shape was found to have a significant effect on the flow field. The velocity at the top and bottom of the cylinder is twice the velocity that seen away from the cylinder.

1. INTRODUCTION

Analytical solutions are generally preferred to study the simple contour conditions of systems. For instance, analytical solutions are the most sought-after options when the modeling leads to a linear differential equation. Nevertheless, analytical solutions cannot obtain exact solutions when the presence of non-linear differential equations is imminent. On the other hand, numerical methods may provide approximate solutions even if the boundary conditions become complex and the fluid flow become transient. With the advent of the most powerful computers capable of performing calculations at relatively higher speeds, there is a rapid development that enabled several researchers to use different numerical methods in fluid flow engineering. Alexandre Joel Chorin introduced the first numerical method for solving incompressible viscous flow problems in 1947.

[1] Corresponding author: Brahmanandam P S
Email: dranandpotula@svecw.edu.in

Numerical and finite difference methods have been used in various applications, such as modeling Navier-Stokes equations for vortex generation, pipe flow, Couette flow, static structural analysis, wave analysis, etc. As far as the ionosphere and atmosphere studies are concerned, understanding viscous effects is crucial for modeling and predicting ionospheric phenomena like plasma convection and ion transport (Potula et al., 2011; Brahmanandam et al., 2012; Brahmanandam et al., 2020; Uma et al., 2016). Understanding viscous effects aids in studying air quality near the surface.

Numerical methods have been adapted to solve many problems and prove cheaper than experimental results. However, since the numerical techniques use approximations, the mathematical models have to be tested for various boundary conditions and governing equations to obtain a reliable solution. A lot of research is being conducted on the stability of such numerical models and the reliability of the solution obtained by these methods (Lin, 1961; Hughes, 1972, and references therein).

Plane Hagen- Poiseuille (after J. L. M. Poiseuille and G. H. L Hagen) flow is broadly defined as a steady and laminar flow of a viscous fluid between two horizontal parallel plates separated by an appropriate distance. In Poiseuille flow, a constant pressure gradient (dp/dx) is applied across the length of the plate flow. It is exemplified by a two-dimensional (2D) velocity profile (v(y)) symmetric about the mid-plane, as shown in Figure 1. From the continuity equation for a flow between two fixed plates, as shown in figure 1, the governing equations are

$$\frac{\partial u}{\partial x}+\frac{\partial v}{\partial y}=0$$

(Since for 1-D flow, if we write Navier- Stokes equations in the x-direction, non-linear convective terms become zero)

$$\text{As v= 0, } \frac{\partial u}{\partial x}=\frac{du}{dx}=0$$

$$\text{u= u(y)}$$

The x-moment equation:

$$\rho\left(u\frac{\partial U}{\partial x}+v\frac{\partial U}{\partial y}\right)=-\frac{\partial P}{\partial x}+\mu\left(\frac{\partial^2 u}{\partial x^2}+\frac{\partial^2 u}{\partial y^2}\right)$$

$$\rho(0)=-\frac{\partial P}{\partial x}+\mu\left(\frac{\partial^2 u}{\partial x^2}+\frac{\partial^2 u}{\partial y^2}\right)$$

$$\frac{\partial P}{\partial x}=\mu\left(\frac{\partial^2 u}{\partial y^2}\right) \quad (1)$$

The y-momentum equation:

$$\rho\left(u\frac{\partial v}{\partial x}+v\frac{\partial v}{\partial y}\right)=-\frac{\partial P}{\partial x}+\mu\left(\frac{\partial^2 v}{\partial x^2}+\frac{\partial^2 v}{\partial y^2}\right)$$

$$\rho(0+0)=-\frac{\partial P}{\partial y}+\mu\,(0+0)$$

$$\frac{\partial P}{\partial y}=0 \quad (2)$$

The z-momentum equation:

$$\rho\left(u\frac{\partial w}{\partial x}+v\frac{\partial w}{\partial y}+W\frac{\partial w}{\partial z}\right)=-\frac{\partial P}{\partial z}+\mu\left(\frac{\partial^2 w}{\partial x^2}+\frac{\partial^2 u}{\partial y^2}\right)$$

$$\rho(0+0+0)=-\frac{\partial P}{\partial z}+\mu\,(0+0)$$

$$\frac{\partial P}{\partial z}=0 \quad (3)$$

From equations 1, 2, and 3, it is obvious that

$$\frac{\partial P}{\partial x}=\mu\left(\frac{\partial^2 u}{\partial y^2}\right),\qquad \frac{\partial P}{\partial y}=0, and\ \frac{\partial P}{\partial z}=0$$

And, it is also clear that $\frac{\partial P}{\partial x}=\mu\left(\frac{\partial^2 u}{\partial y^2}\right)=constant$

The constant is expected to be negative because the pressure must decrease in the flow direction to overcome the resisting wall shear stress. Then applying the double integral to the above equation gives the velocity profile, therefore,

$$u=\frac{1}{\mu}\left(\frac{\partial p}{\partial x}\right)\frac{y^2}{2}+C_1+C_2 \quad (4)$$

Invocation of boundary conditions (at y= ±h; u=0) leads to the following conditions

$$C_1=0 \text{ and } C_2=-\left(\frac{\partial p}{\partial x}\right)\frac{h^2}{2\mu} \quad (5)$$

$$u=-\left(\frac{\partial p}{\partial x}\right)\frac{h^2}{2\mu}\left[1-\frac{y^2}{h^2}\right] \quad (6)$$

Equation 6 is a parabola equation, and that's why the velocity profile of Poiseulle's flow looks like a parabola shape (see figure 1 for more details).

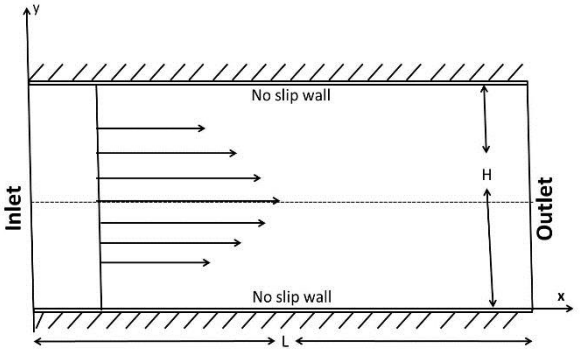

Figure 1. Plane Hagen-Poiseuille flow between two flat plates, where 'L (H)' is the length (height) of the plate

Couette flow is a viscous flow between two parallel plates separated vertically by a considerable distance (Munson et al. 2004). In general, the upper plate moves with some velocity while the bottom plate remains stationary. The Couette flow is two-dimensional in the xy plane. The flow between the two plates is driven by the shear stress exerted on the fluid by the moving plates. A velocity profile is, thus, formed on the flow, as depicted in the following figure. The schematic of Couette flow is presented in Figure 2.

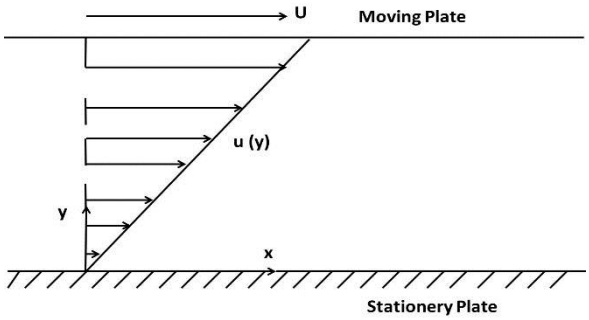

Figure 2. Schematic of Couette flow between two plates

As per as the fundamental governing equations of Couette flow are concerned, incompressible fluid dynamics problems are, in general, described by simple Navier- Stokes (NS equations).

Let us assume both plates are infinitely large in z direction (see figure 2), and, hence, z dependence cannot be considered. Then, applying continuity equation, one can have

$$\frac{\partial U}{\partial x} + \frac{\partial V}{\partial y} + \frac{\partial W}{\partial z} = 0 \tag{7}$$

Navier- Stokes equation in x-direction,

$$\rho\left(\frac{\partial U}{\partial t} + U\frac{\partial U}{\partial x} + V\frac{\partial U}{\partial y} + W\frac{\partial U}{\partial z}\right) = -\frac{\partial P}{\partial x} + \rho g_x + \mu\left(\frac{\partial^2 U}{\partial x^2} + \frac{\partial^2 U}{\partial y^2} + \frac{\partial^2 U}{\partial z^2}\right)$$

$$\frac{d^2u}{dy^2} = 0 \tag{8}$$

Once we integrate the above second order differential equation (8), we get

$$\frac{du}{dy} = C_1$$

Then, the second integration yields, the following equation, such as

$$u(y) = C_1 y + C_2 \tag{9}$$

Invocation of initial (y=0, u=0) and final (y=b, u= V) boundary conditions allow us to have C_2 to be zero. If C_2 value is zero (once implemented in equation 9), then C_1value becomes V/b. And, finally we will have

$$u(y) = V*y/b \tag{10}$$

Equation 5 indicates that the relation between u and y is linear. The above equation can also be written as follows and it can be solved using MATLAB easily

$$u/y = V/b \tag{11}$$

To know the numerical approximation of the above equation, we used a second-order finite difference Crank-Nicolson Scheme in this study because that scheme is an implicit scheme and unconditionally stable and, hence, it is convergent. Usually, the Crank–Nicolson scheme is the most accurate scheme for small-time steps (Abdon Atangana, 2016). On the other hand, the explicit scheme is the least valid and can be unstable, but it is also the easiest to implement and the least numerically intensive. Using the Central difference method, we obtained the velocities at different nodes at different time intervals for several iterations.

2. NEED OF THE STUDY AND ORGANIZATION OF THE ARTICLE

Many analytical and numerical investigations have been carried out on various flows. However, they focus only on single entities (Fredsoe & Sumer, 1997; Benim et al. 2007; Butt & Egbers 2013; Luckachan et al. 2022). Some studies deal only with laminar flow (Park & Kim, 1998; Rajani et al. 2009; Bai & Li 2011; Ganie et al., 2022) or turbulence (Ong et al. 2009; Cao & Tamura 2008; Benim et al. 2007; Young & Ooi 2004). In this work, various flow fields including Poiseuille and Couette flows and their analytical and numerical solutions are discussed.

Further, flow around a cylinder is studied and its analytical and numerical solutions are provided. Most importantly, a simple schematic model is proposed that helps to understand the existence of shear stresses and pressure gradient forces between two plates in opposite directions. As a result, a backflow regime is created within the stream, and this simple model may serve as a source of inspiration for other researchers to continue their work in this exciting field. Still, we believe there is a lot of room for these works, even though we are limiting ourselves to a few types of flows. The future scope of this work is detailed in the final section of this article.

This paper consists of three sections. First, we introduce the importance of analytical and numerical solutions for various flows and the associated equations. Next, results and discussion are included, wherein we thoroughly discuss analytical and numerical solutions of various flows. Most importantly, a schematic model is proposed that helps us to explain the backflow regime in flow. Analytical and numerical flow solutions around a circular cylinder are discussed in the same section. The conclusion summarizes the results and it also contains future scope of these works, which follow the acknowledgments.

3.0 RESULTS AND DISCUSSION

3.1 Analytical and numerical solutions of plane Poiseuille flow– Finite difference method

In the finite difference method, the derivatives will be approximated by finite differences on a grid. To solve a linear value problem of the form $y^{11}= p(x)y^1+ q(x)y+ r(x)$, the following boundary conditions are considered such as $y(x_1)$= alpha and $y(x_2)$= beta.

The plane Poiseuille flow is solved using the finite difference method, for which we have considered the plate separation to be 0.1 and the viscosity μ = 1. The boundary conditions are: x1= 0; alpha= 0; and x2=0; beta= 0. The exact and the numerical (approximate) solutions of plane Poiseuille flow are almost converging, as shown in figure 3.

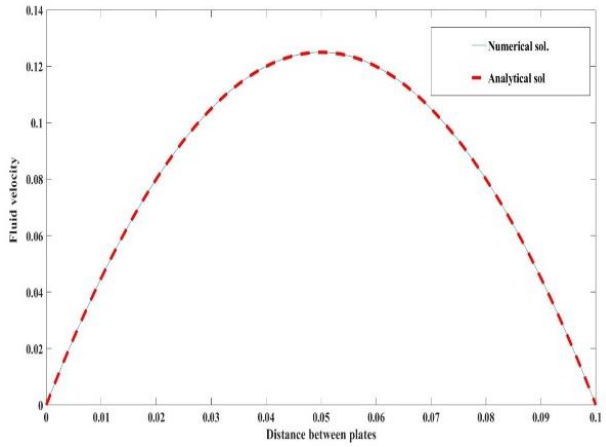

Figure 3. Analytical and numerical solutions of plane Poiseuille flow

3.2 COUETTE FLOW IN DIFFERENT SCENARIOS

3.2.1 Couette flow under different pressure gradient conditions

Couette flow is used to describe shear-driven motion in which the fluid flow is induced by the motion of one of the plates in the channel. As for the technical application of this flow, it is used in fluidics, geophysics and astrophysics. Couette flow theory can be used to measure viscosity and estimate drag in many applications.

We first investigated the behavior of the velocity profile at different pressure gradients. The dimensionless pressure gradients considered here range from -5 to +5 (11 in total) and the resulting velocity profiles are shown in the figure below. Figure 4 shows Couette velocity profiles under different pressure gradients. From this figure, it is clear that the velocity profile increases with favorable dimensionless pressure gradient, similar to the findings of Kuiry and Bahadur (2015) and Muhim Chutia (2018), and references therein.

We also see that the numerical solution converges to the exact solution when the pressure gradient is zero (plane Couette flow). It is also clear that the analytical solution decreases as a linear change between the bottom and top walls when the pressure drop goes to zero. It is also clear that the velocity profile is linear at steady state (see velocity profile with zero pressure gradient in Figure 4).

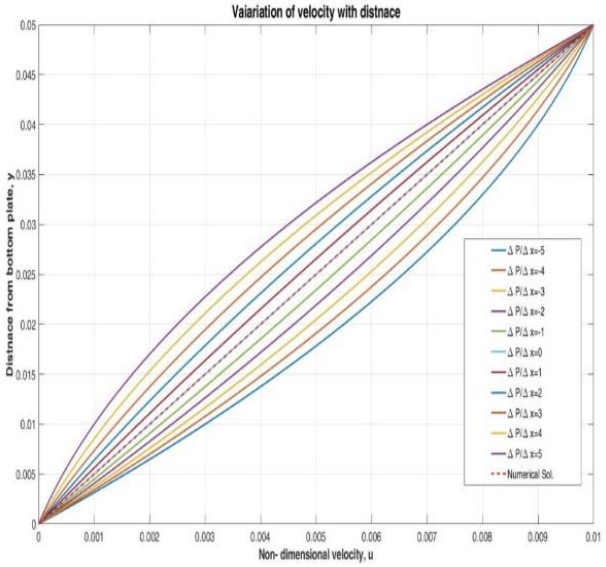

Figure 4. Couette flow velocity profiles under favourable pressure gradient ($\frac{\Delta p}{\Delta x} = -5, -4, -3, -2, -1$), zero pressure gradient ($\frac{\Delta p}{\Delta x} = 0$), **and** adverse pressure gradient ($\frac{\Delta p}{\Delta x} = 1, 2, 3, 4, 5$) conditions

3.2.2 The top plate is moving while the bottom plate is held constant scenario

This section shows the Couette velocity profile for a grid point of 101 and a top velocity of 1 m/s. Figure 5 shows the velocity profile from 0 to 25 seconds. The figure shows that the analytical solution reaches steady state over time as the number of iterations increases. To be precise, it took about 25 seconds to go from transient to steady state. Moreover, the profile appeared to shift towards steady state as the truncation error decreased over time. It has been reported that for an arbitrary Reynolds number of 2000 and an associated error of 0.00458, it took nearly 1000 seconds to reach steady state from transient state (Santos & Chaves, 2019).

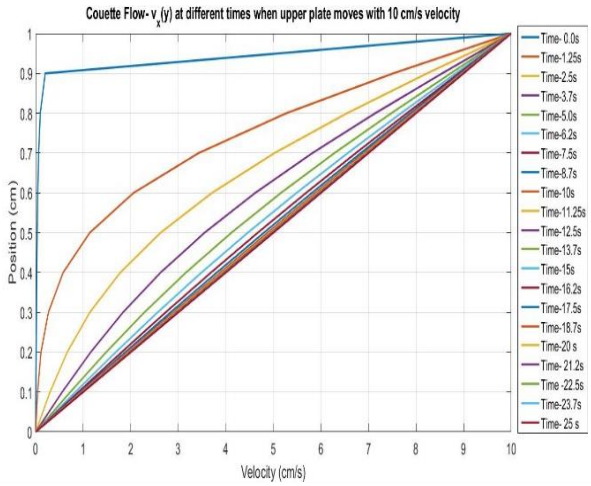

Figure 5. Couette flow when the upper plate is moving

3.2.3 The top plate is held constant while the bottom plate is moving scenario

To verify the effect of the drag force on the liquid from the lower plate, the upper plate remained constant while the lower plate moved at a constant velocity, simulating the Couette flow in different environments. Figure 6 shows velocity profiles at various times from 0 to 25 seconds. It is interesting that the direction of flow is reversed compared to Figure 5, but this is mainly due to liquid resistance through the bottom plate. Interestingly, similar to the velocity profile in Figure 5, it also took almost 25 seconds to reach steady state from transient.

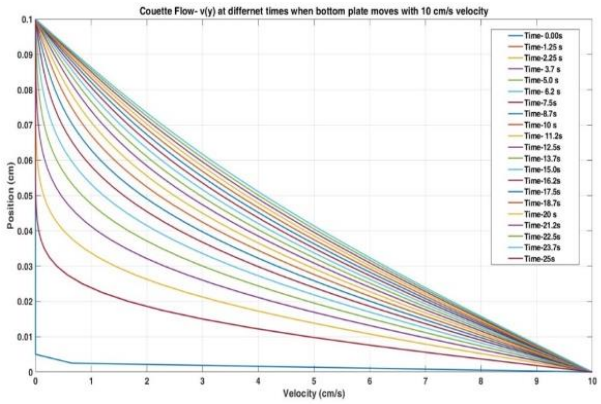

Figure 6. Couette flow when the bottom plate is moving

3.2.4 The top plate is moving and the bottom plate is held constant under adverse pressure gradient condition scenario

Here a special case is shown where the top plate moves at 80 m/s and the bottom plate remains constant under adverse pressure gradient conditions. In this case, it is reasonable to assume that the velocity profile for this scenario exhibits a line similar to the trend shown in Figure 6. However, due to the presence of an adverse pressure gradients, the flow tends to reverse starting at the bottom plate, and this reverse flow condition is known as backflow regime (BFR) or reverse flow reverse (RFR) (Kundu et al., 2016). Figure 7 shows a parabolic velocity profile from the beginning of the top plate to near the bottom plate. It is also possible to see the BFR from this figure.

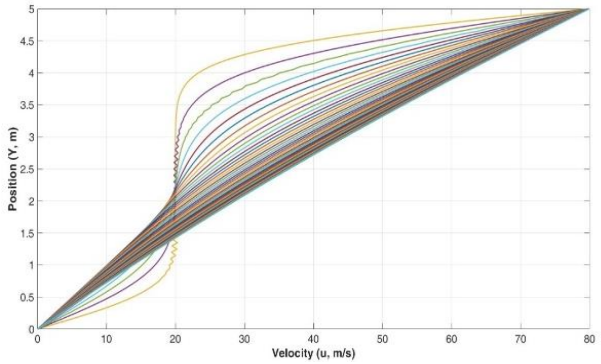

Figure 7. Couette flow under adverse pressure gradients

In such circumstances, there is a competition between the shear stress force (diffusive momentum flux) exerted by the moving plate (which tries to move the fluid from left to the right direction) and pressure gradient force (which tries to move the fluid from right to left), as shown in the following figure. Figure 8 presents a simple schematic model indicating the presence of shear stress and pressure gradient forces on fluid. Further, if the shear stress force completely dominates the pressure gradient force, the velocity profile becomes parabolic, similar to Kundu et al. (2016, see their Figure 9.4a) results.

The schematic model presented in figure 8 shows the moderate dominance of shear stress forces over pressure gradient forces. That's why BFR has occupied nearly 33% of the entire region, as seen in Figure 8. The second option is that if the pressure gradient force dominates the shear stress, one would expect a reverse flow, which can also be found in the research by Kundu et al. (2016, see their Figure 9.4b). Last but not least, when the pressure gradient becomes zero, the velocity profiles would look as in Figure 2 of this article. This similar velocity profile could also be found in the research by Kundu et al. (2016, see their Figure 9.4c).

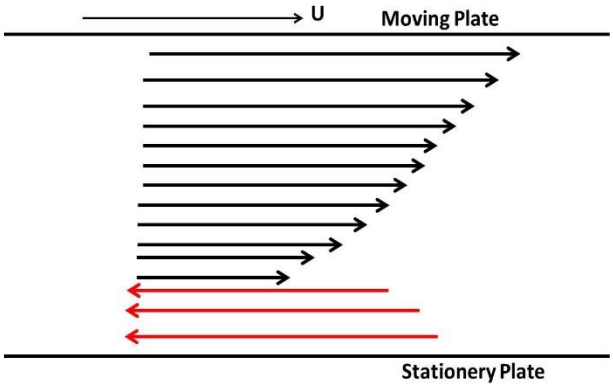

Figure 8. A simple schematic model helps us understand the presence of shear stress and pressure gradient forces between two plates, wherein black arrows (left to right) represent shear stress forces. In contrast, red arrows (right to left) represent pressure gradient forces

3.3 Flows around a circular cylinder

Fluid flow around circular cross-sections is recognized as an important problem in fluid dynamics. Moreover, this is an exciting aspect of research that has attracted researchers for several years (Yuce & Kareem, 2016). Several engineering applications, including bridge piers, offshore structures, and pipelines can, effectively, be modelled as cylinders. The flow around cylinders exhibits many important physical phenomena, such as flow separation, turbulence, and vortex shedding (Yuce & Kareem, 2016, and reference therein). The flow over a circular cylinder is the combination of uniform flow and a doublet, according to Ngo and Gramol (2004).

The superimposed stream function and velocity potential are given by

$$\Psi = \Psi_{\text{Uniform flow}} + \Psi_{\text{doublet}} = U\, r \sin\Theta - K \sin\Theta / r$$

and

$$\Phi = \Phi_{\text{Uniform flow}} + \Phi_{\text{doublet}} = U\, r \cos\Theta + K \cos\Theta / r$$

Since the streamline that passes through the stagnation point has a value of zero (see, figure 10 for further clarification), the stream function on the surface of the cylinder of radius 'a' is then given by

$$\Psi = U\, a \sin\Theta - K \sin\Theta / a = 0$$

This gives the strength of the doublet as

$$K = U\, a^2$$

The stream function and velocity potential for flow past a fixed circular cylinder become

$$\Psi = U\, r(1-(a/r)^2) \sin\Theta$$

and

$$\Phi = U\, r(1+(a/r)^2) \cos\Theta$$

Then, both velocity components (radial and tangential) can be written as

$$V_r = \frac{1}{r}\frac{\partial \Psi}{\partial \theta} = U\left[1 - \frac{a^2}{r}\right]\cos\theta$$

$$V_\Theta = -\frac{\partial \Psi}{\partial r} = -U\left[1 + \frac{a^2}{r}\right]\sin\theta$$

Figure 9 shows both analytical and numerical solutions of velocities over the circular cylinder, from 0 to 360 degrees. The discrepancy between the velocities calculated numerically and analytically is extreme at ~ 90 degrees and ~ 270 degrees, respectively. On the other hand, most surfaces show better agreement with sufficient accuracy. This observed marginal discrepancy may be reduced by modifying the default equation solver settings (for example, by tightening the convergence criteria and increasing the number of iterations), and viscous effects can also affect this discrepency (Ngo & Gramol, 2004). Overall, the analytical and numerical showed moderate to reasonable agreement.

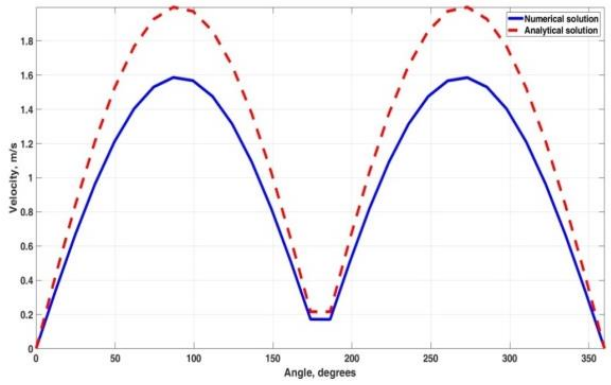

Figure 9. Shows both analytical and numerical solutions of velocities over the circular cylinder, from 0 to 360 degrees

Figure 10 shows velocity vectors superimposed on the velocity magnitudes around the circular cylinder. Here, warmer colors represent faster velocities. The cylinder shape is found to have significantly affected the flow field (Yuce & Kareem, 2016) and the flow smoothly divides and reunites around the cylinder. This case falls into the low speed category because at low speed the smooth fluid flow becomes unstable and at high speed it becomes turbulent.

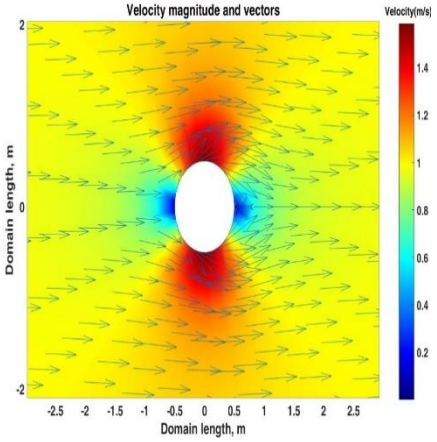

Figure 10. Velocity magnitude and vectors around a circular cylinder

It is obvious that green represents the free stream velocity, which is the velocity that is far from the cylinder. Fluid elements approaching the cylinder directly (at the equator) slow down once they are sufficiently close (shifting to blue color). The fluid element on the upstream side of the cylinder's surface stops moving, or its velocity decreases to zero. It is referred to as a stagnation point. The magnitude of the fluid constituents' velocities increases as they travel above or below the cylinder (shifting to red). Two times as fast as the free stream is the velocity at the top and bottom of the cylinder. Tangential or parallel to the cylindrical surface, velocity exists along the cylinder surface.

4.CONCLUSION AND FUTURE SCOPE

This work presents analytical and numerical solutions for various flows. The salient features of this study are as follows:

a) Exact and numerical solutions of planar Poiseuille flow converge without contradiction.
b) The fluid velocity increases with favorable dimensionless pressure gradient.
c) Couette flows simulated in different scenarios yielded exciting results.
d) If the pressure drop goes to zero, the analytical solution will decrease as a linear change between the bottom wall and the top wall. If the bottom plate is held constant, the flow will be in the opposite direction, mainly due to the drag force on the fluid by the bottom plate.
e) The flow forms a backflow regime when the upper plate moves under adverse/unfavorable

pressure gradient conditions. To describe the backflow regime, we present a simple schematic model that helps to understand the competition between momentum diffusion and pressure gradient forces as to develop a backflow regime. Analytical and numerical solutions for flow over a cylinder are shown.

f) We explained the reasons for marginal discrepancy (at only few places) between.

g) Analytical and numerical solutions. Using the velocity magnitude and velocity vector plot, we observe that the shape of the cylinder has a large effect on the flow field and the velocity at the top and bottom of the cylinder being twice that of the free stream (velocity away from the cylinder).

As far as the future scope of these research works are concerned, the flow field around a cylinder of Reynolds number (Re) ranges from a minimum value (e.g. 10 – laminar flow) to a higher value (5×10^6 – turbulent flow) will be studied. We also focus on examining both analytical and numerical studies such as flows in infinite parallel plates, vertically falling films, flow in rotating tubes, and boundary layers. This will give you more insight into the flow. In addition to the Reynolds number scenario, the flow direction also has a significant impact on the flow dynamics around the cylinder. Since the direction of the free jet can be changed (Zhang et al., 2019), the effect of angle of attack on the flow will be investigated as part of future research.

References:

Abdon Atangana (2016). Method for partial differential equations with beta-derivative, Editor(s): Abdon Atangana, Derivative with a New Parameter, *Academic Press*, pp. 61-94. doi: 10.1016/B978-0-08-100644-3.00004-0

Bai, H., & Li, J. W. (2011). Numerical simulation of flow over a circular cylinder at low Reynolds number. *Advanced Materials Research*, *255*, 942-946. doi: 10.4028/AMR.255-260.942

Benim, A. C., Gul, F., & Pasqualotto, E. (2007, August). Numerical investigation of the role of the inlet swirl velocity profile on decay of swirl in pipe flow. In *Proc. 5th Int. Conf. on Fluid Mechanics and Aerodynamics* (pp. 25-27), Athens, Greece.

Brahmanandam, P. S., G. Uma, J. Y. Liu, Y. H. Chu, N. S. M. P. Latha Devi, and Y. Kakinami (2012), Global S4 index variations observed using FORMOSAT-3/COSMIC GPS RO technique during a solar minimum year, *J. Geophys. Res.*, 117, A09322, doi:10.1029/2012JA017966

Brahmanandam, P. S., Kumar, V. N., Kumar, G. A., Rao, M. P., Samatha, K., & Ram, S. T. (2020). A few important features of global atmospheric boundary layer heights estimated using COSMIC radio occultation retrieved data. *Indian Journal of Physics*, *94*, 555-563. doi:10.1007/s12648-019-01514-7

Butt, U., & Egbers, C. (2013). Aerodynamic characteristics of flow over circular cylinders with patterned surface. *International Journal of Materials, Mechanics and Manufacturing*, *1*(2), 121. doi: 10.7763/IJMMM.2013.V1.27

Cao, S., & Tamura, Y. (2008). Flow around a circular cylinder in linear shear flows at subcritical Reynolds number. *Journal of wind engineering and industrial aerodynamics*, *96*(10-11), 1961-1973. doi:10.1016/j.jweia.2008.02.041.

Fredsøe, J., & Sumer, B. M. (1997). Scour at the round head of a rubble-mound breakwater. *Coastal engineering*, *29*(3-4), 231-262. doi:10.1016/S0378-3839(96)00025-7

Ganie, A. H., Memon, A. A., Memon, M. A., Al-Bugami, A. M., Bhatti, K., & Khan, I. (2022). Numerical analysis of laminar flow and heat transfer through a rectangular channel containing perforated plate at different angles. *Energy Reports*, *8*, 539-550.. doi: 10.1016/j.egyr.2021.11.232.

Hu, J., Munson, C. L., & Silver, E. A. (2004). A Modified Silver-Meal Heuristic for Dynamic Lot Sizing under Incremental Quantity Discounts. *The Journal of the Operational Research Society*, 55(6), 671–673. http://www.jstor.org/stable/4101973

Hughes, T. H. (1972). Variable Mesh Numerical Method for Solving the Orr- Sommerfeld Equation. *The Physics of Fluids*, *15*(5), 725-728. doi: 10.1063/1.1693974

Kuiry, D. R., & Bahadur, S. (2015). Steady MHD flow of viscous fluid between two parallel porous plates with heat transfer in an inclined magnetic field. *Journal of Scientific Research*, *7*(3), 21-31. doi: 10.3329/jsr.v7i3.22574

Kundu, P. K., Cohen, I. M., & Dowling, D. R. (2016). Fluid Mechanics 6th ed. ISBN: 9780124059351.

Lin, C. C. (1961). Some mathematical problems in the theory of the stability of parallel flows. *Journal of Fluid Mechanics*, *10*(3), 430-438. doi:10.1017/S0022112061001025

Luckachan, K. G., Raja Sekar, K., Srikrishnan, A. R., & Kannan, R. (2022). Transient vortex shedding behaviour of non-reacting flow over V-gutter bluff bodies with a central slit. *International Journal of Ambient Energy*, *43*(1), 8686-8696. doi:10.1080/01430750.2022.2102070.

Muhim Chutia (2018). Effect of variable thermal conductivity and the inclined magnetic field on MHD plane Poiseuille flow in a Porous channel with non-uniform plate temperature, *Journal of Computational & Applied Research*. doi:10.22061/jcarme.2017.1620.1137

Ngo C.C., & Gramol, K. C. (2004). 7th Chapter -Incompressible and Inviscid Flow, *Multimedia Engineering Flud Mechancis*. Archieved from http://www.ecourses.ou.edu/cgi-bin/ebook.cgi?doc&topic=fl&chap_sec=07.4&page=theor

Nikushchenko, D., Pavlovsky, V., & Nikushchenko, E. (2022). Analytical Solutions for Simple Turbulent Shear Flows on a Basis of a Generalized Newton's Law. *Polymers*, *14*(16), 3308. doi: 10.3390/polym14163308.

Ong, M. C., Utnes, T., Holmedal, L. E., Myrhaug, D., & Pettersen, B. (2009). A numerical study on near-bed flow mechanisms around a marine pipeline close to a flat seabed including estimation of bedload sediment transport. *Proceedings of Coastal Processes 2009*, 163-175. Archived from https://www.witpress.com/elibrary/wit-transactions-on-ecology-and-the-environment/126/20640

Park, J. S., & Kim, M. H. (1999). Combustion Characteristics of Plasma Jet Ignition on LPG-Air Mixture in Laminar Flow Field, *Transactions of the Korean Society of Automotive Engineers*, 7, 6869. https://koreascience.kr/article/JAKO199910102414243

Potula, B. S., Chu, Y. H., Uma, G., Hsia, H. P., & Wu, K. H. (2011). A global comparative study on the ionospheric measurements between COSMIC radio occultation technique and IRI model. *Journal of Geophysical Research: Space Physics*, *116*(A2), A02310, doi:10.1029/2010JA015814.

Rajani, B. N., Kandasamy, A., & Majumdar, S. (2009). Numerical simulation of laminar flow past a circular cylinder. *Applied Mathematical Modelling*, *33*(3), 1228-1247. doi:10.1016/j.apm.2008.01.017

Santos, G. B., & Chaves, M. B. (2019). Application of the finite difference method for numerical simulation of the Couette Flow, *25th ABCM Intl. Conference of Mechanical Engineering*, October 202-25, Brazil. doi:10.26678/ABCM.COBEM2019.COB2019-0537

Strikwerda, J. C. (2004). *Finite Difference Schemes and Partial Differential Equations*, 2nd edition, Society for Industrial and Applied Mathematics (SIAM), Philadelphia, USA, 2004. doi:10.1137/1.9780898717938

Uma, G., Brahmanandam, P. S., & Chu, Y. H. (2016). A long-term study on the deletion criterion of questionable electron density profiles caused by ionospheric irregularities – COSMIC radio occultation technique. *Advances in Space Research*, 57(12), 2452–2463. doi:10.1016/j.asr.2016.03.034

Young, M. E., & Ooi, A. (2004, December). Turbulence models and boundary conditions for bluff body flow. In *Proc. 15th Australian Fluid Mechanics Conf*. 13-17 December. Archived from https://www.aeromech.usyd.edu.au/15afmc/proceedings/papers/AFMC00158.pdf

Yuce, M. I., & Kareem, D. A. (2016). A numerical analysis of fluid flow around circular and square cylinders. *Journal - American Water Works Association*, *108*(10), E546-E554. https://www.jstor.org/stable/9000520

Zhang, L., Mao, X., & Ding, L. (2019). Influence of attack angle on vortex-induced vibration and energy harvesting of two cylinders in side-by-side arrangement. *Advances in Mechanical Engineering*, *11*(1), 1687814018822598. doi:10.1177/1687814018822598

Venkat Rao Kanuri
Department of Mathematics,
Koneru Lakahmaiah Education Foundation (KLEF),
Deemed to Be University,
Vaddeswaram,
&
Department of Mathematics,
SRKR Engineering College(A),
Bhimavaram-534204, A.P, India
Andhra Pradesh, India.
k.ravi.msc@gmail.com
ORCID 0000-0003-2364-5074

M. S. R. Murthy
Department of mathematics
Vishnu Institute of Technology (A)
Vishnupur, Bhimavaram- 534202
Andhra Pradesh
India.
murthy.m@vishnu.edu.in
ORCID 0000-0001-6301-0554

K.V.Chandra Sekhar
Dept. of Mathematics,
Koneru Lakahmaiah Education Foundation (KLEF),
Deemed to Be University,
Vaddeswaram,
Andhra Pradesh,
India.
chandu_fed@kluniversity.in
ORCID 0000-0002-8112-2442

P. S. Brahmanandam
Department of Physics
Shri Vishnu Engineering College for Women (A)
Vishnupur, Bhimavaram- 534202
Andhra Pradesh, India.
dranandpotula@svecw.edu.in
ORCID 0000-0001-9777-3496